

Electric field dynamics at a charged point

Mikhail A. Berkovsky and James W. Dufty

Department of Physics, University of Florida, Gainesville, Florida 32611

Annette Calisti, Roland Stamm, and Bernard Talin

*Equipe Diagnostics dans les Plasmas, URA 773, Université de Provence,
Centre de St. Jérôme 13397 Marseille Cedex 13, France*

(Received 25 April 1996)

The autocorrelation function for the electric field at an impurity ion in a plasma is considered. A simple model is constructed that preserves the exact short time dynamics and the long time global constraint of a given self-diffusion coefficient. The input required is the initial value of the autocorrelation function and its derivatives, and the self-diffusion coefficient. These are calculated from the hypernetted chain equations for correlation functions and a “disconnected” approximation for the self-diffusion coefficient. A comparison of the predictions of the model for the electric field autocorrelation function with results from molecular dynamics simulation shows good agreement over a wide range of plasma coupling, impurity ion charge, and impurity ion mass. This provides justification for a simple interpretation of electric field dynamics in terms of three collective modes. [S1063-651X(96)00309-1]

PACS number(s): 52.25.Vy, 52.25.Gj, 52.65.-y, 05.40.+j

I. INTRODUCTION

An impurity ion embedded in a plasma serves as an important probe of charged particle dynamics through both its radiative and transport properties. The dominant coupling between the impurity ion and the surrounding plasma is through the total electric field of the plasma, $\mathbf{E}(t)$, at the ion (force on a charged ion, dipolar coupling to both neutral and charged ions). Determination of the probability distribution for a chosen field value in an equilibrium plasma (the “microfield distribution”) is a well-studied problem with accurate and practical means for calculation [1]. In contrast, the dynamics of the electric field is not well understood even at a qualitative or phenomenological level. Recently, some progress has been made for the case of electric fields at a neutral point [2–5]. Detailed calculations and simulations of the electric field dynamics as a function of time and initial field value at a neutral point [6] show a number of unexpected features: long time algebraic decay, a possible increase at short times, and qualitative failure of the stochastic model microfield method [7]. These results show that some care must be used in the representation of field dynamics in more complex analyses such as spectral line broadening calculations.

The objective here is to extend these studies of electric field dynamics to the case of charged impurity ions. The physics is quite different from that for the neutral case since the presence of the charged ion significantly changes the charge distribution of the plasma in the vicinity of the ion. As a first study, we limit attention to the simplest dynamical property, the electric field autocorrelation function $C(t) = \langle \mathbf{E}(t) \cdot \mathbf{E} \rangle / \langle E^2 \rangle$, where the brackets denote an equilibrium ensemble average. A simple model is constructed to incorporate the most important symmetries of the correlation function and its relationship to structural and transport properties. For example, the time integral of $C(t)$ must vanish exactly as a consequence of the field being proportional to

the total force on the ion. For similar reasons, there is a simple exact relationship to the ion velocity autocorrelation function, $D(t) \equiv \langle \mathbf{v}_0(t) \cdot \mathbf{v}_0 \rangle / \langle v_0^2 \rangle$, and consequently to the self-diffusion coefficient D through an exact Green-Kubo relation. Finally, effects of the induced charge distortion near the impurity ion are incorporated through the exact initial condition and first two time derivatives of $C(t)$ at $t=0$.

The model is constructed from a formally exact equation for $D(t)$. This equation describes the linear response of the ion to an initial perturbation of its velocity, and provides a clear interpretation of the dynamics as damped oscillatory motion in a viscoelastic medium. The complex many-body dynamics is hidden in a “memory” function which is approximated here by simple exponential relaxation. The time scale for this relaxation is fixed by the above-mentioned exact relationship between $D(t)$ and the self-diffusion coefficient D . The resulting equation can be solved to determine both $D(t)$ and $C(t)$ as a function of the self-diffusion coefficient and the initial data. The latter are expressed as integrals of the time independent correlation functions for the charge distribution around the ion and are computed here using the HNC integral equations [8]. The self-diffusion coefficient is calculated using the “disconnected” approximation [9]. None of these approximations implies *a priori* any limitations with respect to plasma coupling strength, ion charge, ion mass, or time scale. Consequently, the model is a good candidate for the description of electric field dynamics over a wide range of conditions.

The time dependence of this model can be expressed as a linear combination of three exponentials, or modes, allowing a simple interpretation of the relevant plasma excitations responsible for electric field dynamics. At weak coupling all three modes represent purely damped excitations, while at strong coupling there is one damped mode and a complex conjugate pair of damped propagating modes. The conditions of “weak” or “strong” coupling depend on plasma coupling, charge, and mass. To limit the parameter space, we

consider the simplest case of a one component plasma (OCP) with ions of the same sign charge in the classical limit. The relevant parameters are then the OCP coupling constant $\Gamma = \beta q^2/a$, the charge ratio q_0/q , and the mass ratio m_0/m , where a is the ion sphere radius, $\beta = 1/k_B T$, and parameters with subscript 0 refer to the impurity ion. Also, we consider both a OCP with Coulomb interactions and one with screened interactions. Density and temperature conditions are limited to the experimentally interesting case of screening by nondegenerate, weakly coupled electrons [10]. The case of a quantum plasma with charges of opposite sign from that of the impurity, and its connection to the problem of stopping power [11], will be discussed elsewhere.

The approximation described here for $C(t)$ is a special case of a more comprehensive approximation constructed for calculating general functions of $\mathbf{E}(t)$ that cannot be expressed in terms of $C(t)$ alone [12]. An important objective and emphasis of that work was to calculate the effects of ion motion on spectral line broadening by plasmas. Subsequent applications have demonstrated the importance of ion motion effects and the good agreement between that model and computer simulations of spectral lines [13]. The objective of the present work is to isolate the simplest features of electric field dynamics from the complexities of that general context for a clear interpretation, analysis, and comparison with computer simulations as a function of the above parameters. Details of the simulation method are described in the next section.

In the next section, the model is described briefly and its predictions analyzed for the case of $q_0/q = m_0/m = 1$. The three modes of excitation are studied as a function of Γ . Comparison with computer simulation results shows good agreement even at strong plasma coupling for both Coulomb and screened interaction. In Sec. III the dependence of the modes on q_0/q and m_0/m is considered. The results are summarized in the final section and a practical means for estimating the diffusion coefficient from simulation data using this model is proposed.

II. A SIMPLE MODEL

The system considered is an impurity ion of mass m_0 and charge q_0 at equilibrium with a fully ionized plasma of point (structureless) ions. The electric field at the impurity ion due to the plasma constituents is given by

$$\mathbf{E} = \sum_{\alpha} \sum_{i=1}^{N_{\alpha}} \mathbf{e}_{\alpha}(\mathbf{r}_i - \mathbf{r}_0) + \mathbf{E}_b, \quad (1)$$

where N_{α} is the number of ions of species α , $\mathbf{e}_{\alpha}(\mathbf{r}_i - \mathbf{r}_0)$ is the field due to the plasma ion at a distance $\mathbf{r}_i - \mathbf{r}_0$ from the impurity ion, and \mathbf{E}_b is the field from the uniform neutralizing background charge. The equilibrium autocorrelation function is defined by

$$C(t) \equiv \langle \mathbf{E}(t) \cdot \mathbf{E} \rangle / \langle E^2 \rangle, \quad (2)$$

where the brackets $\langle \rangle$ denote an equilibrium Gibbs ensemble average. As noted in the Introduction, this function plays a central role in many theories of radiative processes in plas-

mas. A closely related function relevant for transport properties is the velocity autocorrelation function

$$D(t) = \langle \mathbf{v}_0(t) \cdot \mathbf{v}_0 \rangle / \langle \mathbf{v}_0^2 \rangle, \quad (3)$$

where \mathbf{v}_0 is the impurity ion velocity. The correlation function $C(t)$ measures fluctuations in a collective property of the OCP, while $D(t)$ measures fluctuations in a single particle property. However, they are related directly by Newton's first law,

$$\frac{\partial^2 D(t)}{\partial t^2} = -\omega_0^2 C(t), \quad \omega_0^2 = (\beta q_0^2 / 3m_0) \langle E^2 \rangle. \quad (4)$$

The interpretation of our model is more direct in terms of $D(t)$. First, a formally exact equation is derived using the projection operator technique (see Appendix A),

$$\frac{\partial^2 D(t)}{\partial t^2} + \omega_0^2 D(t) + \int_0^t d\tau M(t-\tau) \frac{\partial D(\tau)}{\partial \tau} = 0, \quad (5)$$

$$M(0) = \omega_1^2 - \omega_0^2, \quad \omega_1^2 = \langle \dot{E}^2 \rangle / \langle E^2 \rangle, \quad (6)$$

where $\beta \equiv k_B T$. Equation (5) describes the impurity ion dynamics as oscillations in a viscoelastic medium, where the characteristic frequency is ω_0 and a frequency dependent damping given by the Fourier transform of $M(t)$. All many-body effects of the medium on the impurity ion that are not explicit in (5) are contained in the detailed form of $M(t)$ [15]. Our fundamental assumption here is that it is sufficient to include only the magnitude of this function through its exact initial value $M(0)$ and a characteristic time scale for its decay [16]. Consequently, $M(t)$ is approximated by

$$M(t) \rightarrow M(0) e^{-\lambda t}. \quad (7)$$

The precise form for λ is fixed by the Green-Kubo expression for the self-diffusion coefficient D in terms of the velocity autocorrelation function [15],

$$\beta m_0 D = \int_0^{\infty} dt D(t). \quad (8)$$

Use of (5) with (7) to determine the right side of (8) gives the identification [see Eq. (D3) of Appendix D],

$$\lambda = (\omega_1^2 / \omega_0^2 - 1) / (\beta m_0 D). \quad (9)$$

Equations (5)–(7) and (9) define the approximate model for $D(t)$ and, through (4), the electric field autocorrelation function. By construction, $D(t)$ and $C(t)$ determined in this way are exact through orders t^4 and t^2 , respectively, at short times. Furthermore, the exact time integrals of $C(t)$ and $D(t)$ are assured through (4) and (8). The input data ω_0 , ω_1 , and D might be taken directly from computer simulation. Alternatively, as discussed below, additional independent approximations may be introduced to allow practical calculation of these parameters.

To interpret these parameters, consider conditions such that $\lambda / \omega_0 \gg 1$. Then $M(t)$ decays rapidly in Eq. (5) and the equation simplifies to

$$\frac{\partial^2 D(t)}{\partial t^2} + \omega_0^2 D(t) + \gamma \frac{\partial D(t)}{\partial t} = 0, \quad (10)$$

$$\gamma = (\beta m_0 D) \omega_0^2. \quad (11)$$

The damping constant relative to the characteristic frequency, γ/ω_0 , determines whether the solutions are a pair of oscillatory functions (underdamped), or two real exponential functions (overdamped). This is controlled by the dependence on q_0/q , m_0/m , and Γ as illustrated in the following. More generally, if λ/ω_0 is not large the medium exhibits ‘‘memory’’ and the damping is modified on time scales of the order of λ^{-1} . Thus there are only three parameters (frequencies) that completely characterize the dynamics of the model, ω_0 , γ , and λ .

It is straightforward to calculate the solution to (5) by Laplace transform, yielding $D(t)$ and $C(t)$ as the sum of three exponentials,

$$D(t) = \sum_{i=1}^3 D_i e^{Z_i t}, \quad C(t) = \sum_{i=1}^3 C_i e^{Z_i t}, \quad (12)$$

where the coefficients D_i and C_i are given by

$$D_i = -(\omega_0/Z_i)^2 C_i, \quad (13)$$

$$C_1 = (\lambda + Z_1) Z_1 (Z_3 - Z_2) / \Delta,$$

$$C_2 = (\lambda + Z_2) Z_2 (Z_1 - Z_3) / \Delta,$$

$$C_3 = (\lambda + Z_3) Z_3 (Z_2 - Z_1) / \Delta,$$

$$\Delta \equiv (Z_1 - Z_2)(Z_2 - Z_3)(Z_3 - Z_1), \quad (14)$$

and the $\{Z_i\}$ are solutions to the cubic equation,

$$Z^3 + \lambda Z^2 + \omega_1^2 Z + \lambda \omega_0^2 = 0. \quad (15)$$

Depending on the values of λ , ω_0 , and ω_1 , the solutions may be real or complex.

To evaluate the quality of the predictions from this model we have performed corresponding molecular dynamics simulations for comparisons. Such simulations have been used recently to provide statistical information about static as well as dynamic properties of electric fields for both charged [14] and neutral points [6]. As for standard molecular dynamics simulations for neutral particles, a few hundred particles interacting via a screened Coulomb potential move in a cubic box with periodic boundary conditions, maintaining the system in a stationary state of fixed temperature and density. The results referred to as the ‘‘screened case’’ correspond to a Debye screening length [10]. The results referred to as the ‘‘Coulomb case’’ are represented as the limit of a very large screening length (typically one-half the system size). These latter results have been checked against those for the pure Coulomb case (no screening) using Ewald sums instead of the simple periodic boundary conditions, for both the pair correlation function and the electric field autocorrelation function. There are specific problems arising from the calculation of the field at a single impurity ion when $q_0 \neq q$ and $m_0 \neq m$ due to the poor statistics of a single test particle history for each simulation. This increases the computer time

TABLE I. Γ dependence of ω_0 , ω_1 , and D_* for Coulomb interaction and screened interaction ($\kappa a = 1$); $q_0 = q$ and $m_0 = m$. Diffusion coefficients D_* and D_*^{scr} are given in units of $\omega_p a^2$.

Γ	ω_0	ω_0^{scr}	ω_1	ω_1^{scr}	D_*	D_*^{scr}
0.2	0.577	0.559	34.00	36.97	33.51	53.90
0.5	0.577	0.544	9.767	11.07	5.932	8.713
1	0.577	0.530	4.436	5.137	1.893	2.645
2	0.577	0.517	2.443	2.760	0.681	0.904
5	0.577	0.502	1.528	1.568	0.216	0.267
10	0.577	0.493	1.268	1.202	0.115	0.131

but the strong coupling conditions are a compensating feature. For example, the local changes induced by the test particle for $q_0/q > 1$ lead to more rapid convergence of the electric field correlation function than for $q_0/q < 1$.

The analysis to this point applies for arbitrary plasma composition. To illustrate the physical content of the model we consider the special case of a one component plasma with an impurity ion of the same mass and charge as those for the plasma ions. In this case there is only one dimensionless parameter characterizing the plasma state condition, $\Gamma \equiv q^2 \beta / a$, where $a \equiv (3n/4\pi)^{1/3}$ is the average interparticle distance (ion sphere radius), and n is the plasma density. Table I shows the Γ dependence of ω_0, ω_1 (in units of the OCP plasma frequency ω_p , defined by $\omega_p^2 \equiv 4\pi n q^2 / m$), and $D_* = D / (a^2 \omega_p^2)$ for both Coulomb and screened interactions. The calculation and approximations used are described in Appendix B. From these results it follows that γ/ω_0 varies inversely with Γ . Consequently, we expect underdamped oscillatory motion at strong coupling and purely damped modes at small Γ .

Consider first the case of Coulomb interactions. Figure 1 shows the real and imaginary parts of the three solutions to (15) as a function of Γ . For small Γ all three are real and negative, representing purely damped excitations. The modes

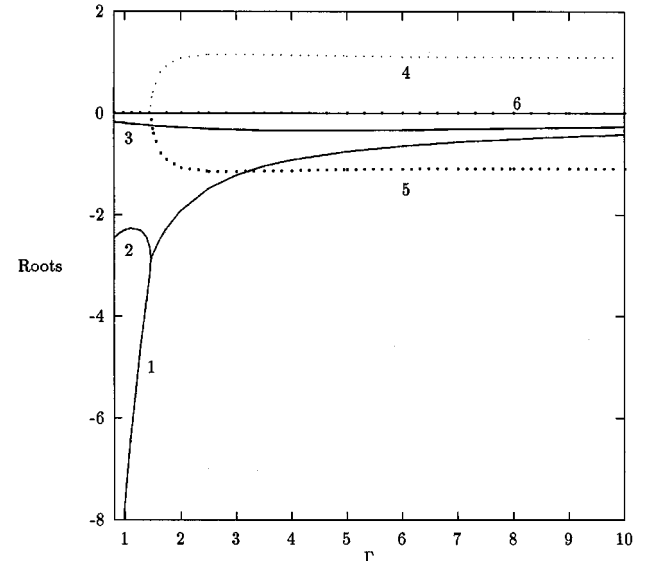


FIG. 1. Solutions to Eq. (15) for the model of Coulomb interaction with $q_0 = q$ and $m_0 = m$. Curves 1–3—real parts of solution; curves 4–6—imaginary parts.

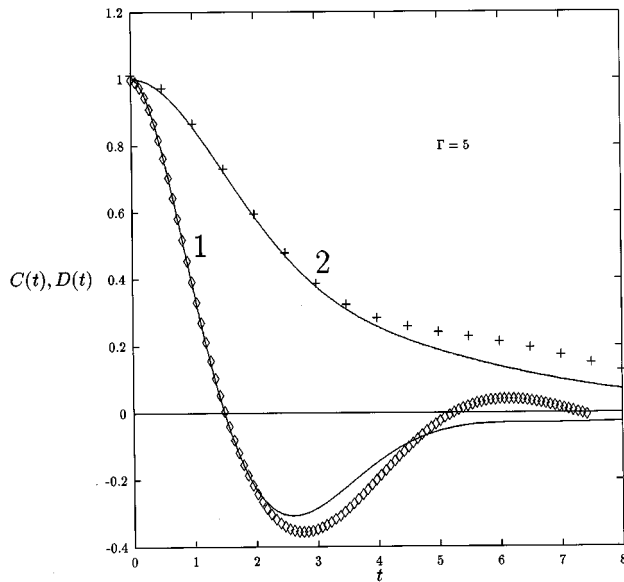


FIG. 2. Time dependence of the electric field correlation function (curve 1) and the velocity autocorrelation function (curve 2) for the case of Coulomb interaction with $\Gamma = 5$. Time is given in units of ω_p^{-1} . Points: MD simulation results.

are widely separated in magnitude so that at times long compared to the inverse plasma frequency the dynamics of $C(t)$ and $D(t)$ is governed by a single exponential in time, with a relaxation time $\sim 5/\omega_p$. The amplitude of this mode in $C(t)$ is negative, to ensure that the time integral of the correlation function vanishes. At very short times all three modes contribute, as is required in order to fit the exact initial t^2 behavior of both correlation functions. Thus the electric field autocorrelation function decreases from unity according to Gaussian-like decay for very short times, followed by two exponentials with the positive amplitude dominating at intermediate times and the negative amplitude dominating at long times. This qualitative behavior persists as Γ increases until a critical value, $\Gamma \sim 1.5$, is reached at which the two most strongly damped modes coalesce to form a complex conjugate pair of damped propagating modes. The frequency of oscillation increases with Γ rapidly to a saturation value at the plasma frequency. The damping of these propagating modes decreases to become comparable with that of the third purely damped mode. Thus for $\Gamma > 1.5$ the dynamics of $C(t)$ and $D(t)$ is qualitatively different from that at small Γ , except for asymptotically small times. This is illustrated in Fig. 2 for the strong coupling value of $\Gamma = 5$. Also shown are the results from computer simulation. The agreement is excellent at short times and quite reasonable at longer times. Generally, the agreement is better at $\Gamma = 1$ with significant differences apparent for $\Gamma > 10$. In spite of the direct relationship of $C(t)$ to $D(t)$, these figures show that the dynamical features at stronger coupling are displayed more directly through the electric field autocorrelation function. For $\Gamma < 1.5$ these differences are not so strong.

The results are qualitatively similar for screened interactions. Figure 3 shows the results for the same strong coupling conditions as in Fig. 2, except now for Debye screened interactions. Finally, Fig. 4 compares the Coulomb and screened cases with the corresponding molecular dynamics

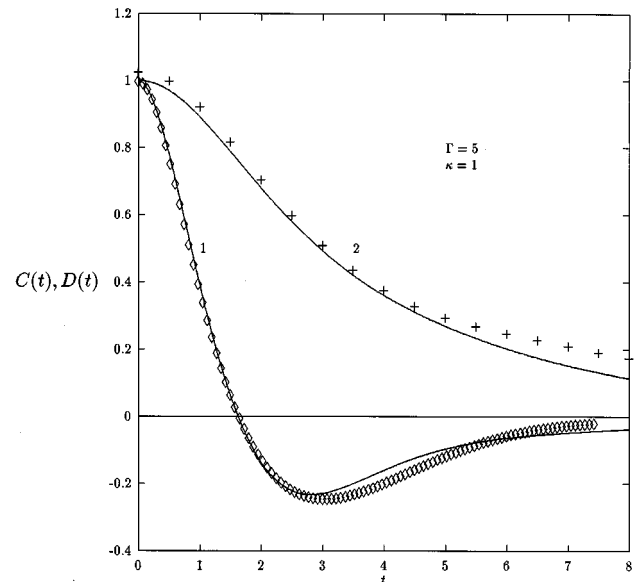


FIG. 3. Same as Fig. 2 for the screened interaction with screening parameter $\kappa = 1$ (κ is given in units of inverse ion spacing, a^{-1}). Points: MD simulation results.

results at the extreme coupling of $\Gamma = 10$. While there are significant differences relative to the simulation results at longer times, the model is still accurate up to $t \sim 3\omega_p^{-1}$ and preserves the qualitative effects of screening at all times.

III. CHARGE AND MASS DEPENDENCE

The analysis of the preceding section suggests that this simple model captures the dominant mechanisms responsible for electric field dynamics. In this section we consider effects due to variation of the impurity ion charge and mass relative to that of the OCP ions. Attention is restricted to the more

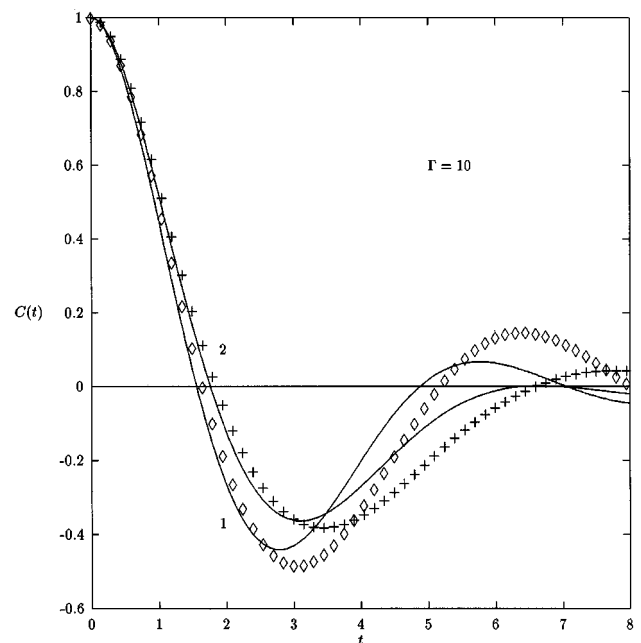


FIG. 4. Time dependence of electric field correlation function for the model of Coulomb interaction (curve 1) and Debye screening ($\kappa = 1$, curve 2) at $\Gamma = 10$. Points: MD simulation results.

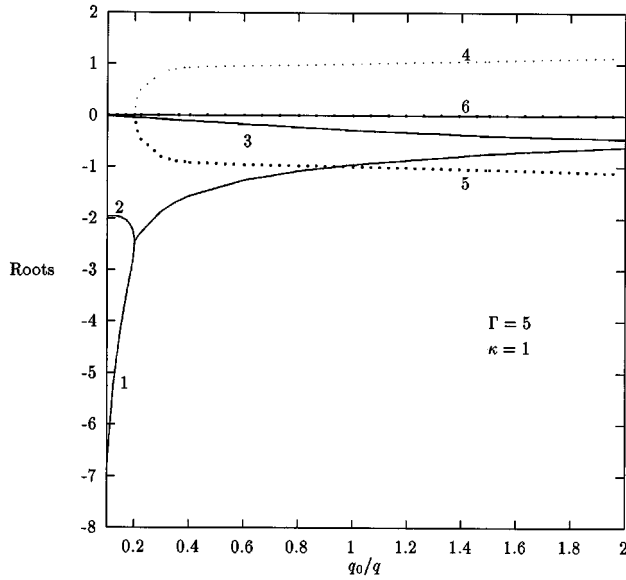


FIG. 5. Solutions to Eq. (15) as a function of q_0/q for the model of screened interaction at $\Gamma=1$ and $\kappa=1$; $m_0=m$.

realistic case of screened interactions. This dependence can be understood in terms of the model through the corresponding dependence of the three parameters ω_0 , γ , and λ . From the results of Appendix B it is seen that the dominant dependence (in units of the plasma frequency) is given by $\omega_0 \propto (mq_0/m_0q)^{1/2}$, $\gamma/\omega_0 \propto (mq/m_0q_0)^{1/2}\Gamma^{-1}$, and $\lambda/\omega_0 \propto (\gamma/\omega_0)\Gamma^{-3/2}$. This dimensional analysis confirms the results of the preceding section, that the damping is weakest at strong coupling, $\Gamma > 1$. Similarly, the damping is expected to decrease with increasing m/m_0 and increasing q/q_0 , although it is via a weaker square root dependence.

Consider first the variation with charge at $m_0/m=1$. For large Γ only small values of q_0 are required to span the domain from weak to strong damping; conversely, for small values of Γ large values of q_0/q are required to reach strong coupling. In the former case ω_0^2 remains small and plays little role in the qualitative features of the modes. In this case the dependence of the modes on q_0/q at fixed Γ should be similar to their dependence on Γ at fixed q_0/q in Fig. 1. Figure 5 confirms this expectation for the case of $\Gamma=5$. As expected for this value of Γ the modes show the strong coupling oscillatory behavior for all $q_0/q \geq 0.2$. However, for small Γ it is necessary to consider large values of q_0/q and the effects of variation of ω_0^2 with the charge become important. This is illustrated in Fig. 6 for $\Gamma=0.2$. Since Γ is decreased by a factor of 25 relative to Fig. 5 a corresponding scale change of the charge is required to show the transition to strong coupling. Note that now λ is large and there are qualitative differences between Figs. 5 and 6. For example, in Fig. 6 the smaller two modes combine to form a propagating pair for increasing q_0/q , while it is the larger two modes that combine in Fig. 5. Figure 7 shows the field correlation function for $\Gamma=5$ and the two cases of $q_0/q=0.2$ and 2. The former corresponds to weak coupling (three real modes) with monotonic crossover from a short time positive domain to a larger long time negative domain, as discussed in Sec. II above. The latter corresponds to strong coupling with two oscillatory and one damped mode. Differences be-

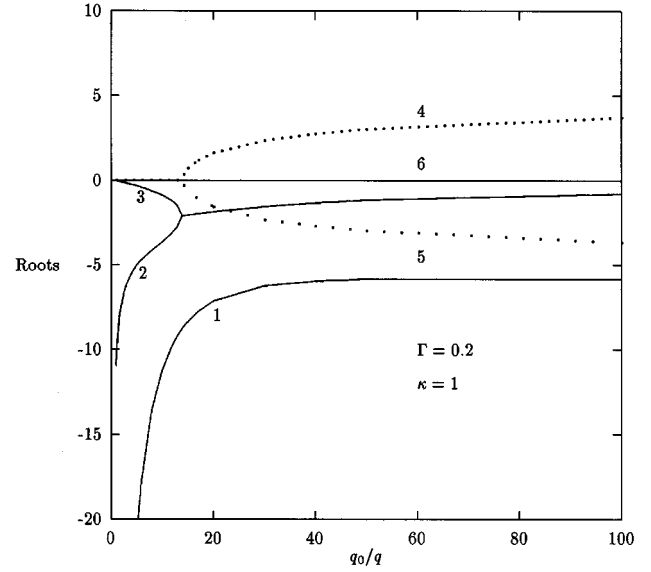


FIG. 6. Same as Fig. 5 at $\Gamma=0.2$ and $\kappa=1$.

tween the model and computer simulation results are expected in this case since the coupling is comparable to that of Fig. 4.

The above variations with respect to Γ and q_0/q reflect different degrees of coupling between the impurity ion and the OCP. The mass dependence is somewhat different. It appears in the same way as for q_0/q in both γ/ω_0 and λ/ω_0 but with an inverse relationship for ω_0 . It is instructive to consider first the limit $m_0/m \rightarrow \infty$. The analysis is given in Appendix D. First, the self-diffusion coefficient approaches a finite limit given by an exact Green-Kubo relation that is applicable only for infinite m_0 ,

$$D^{-1} \rightarrow \beta^2 q_0^2 \langle E^2 \rangle \int_0^\infty dt \lim_{m_0/m \rightarrow \infty} C(t). \quad (16)$$

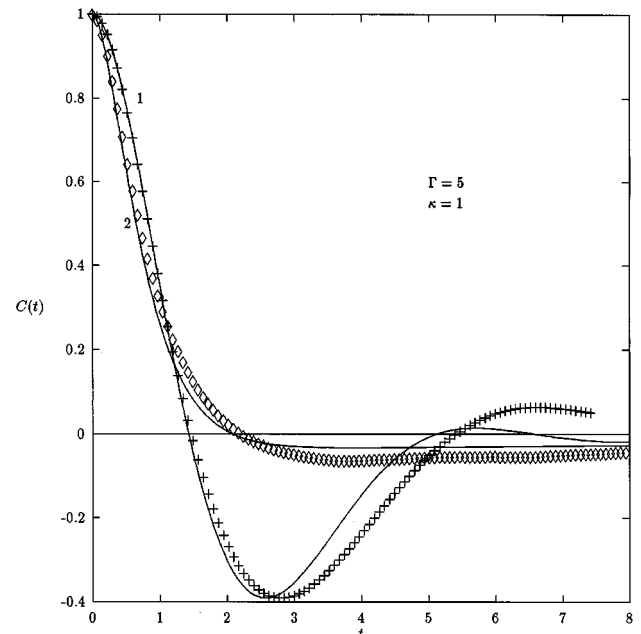


FIG. 7. Time dependence of the electric field correlation function for the case of screened interaction with $\Gamma=5$ and $\kappa=1$. Curve 1— $q_0=2q$; curve 2— $q_0=0.2q$. Points: MD simulation results.

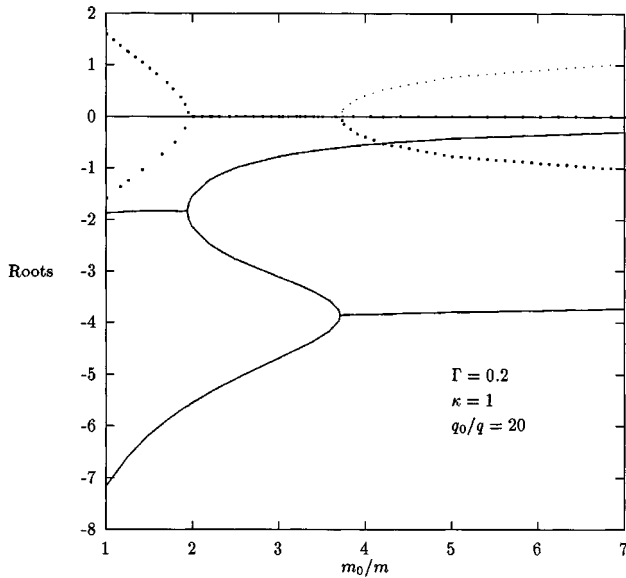


FIG. 8. Solutions to Eq. (15) for the model of screened interaction with $\Gamma = 0.2$, $\kappa = 1$, and $q_0/q = 20$. Solid lines represent real parts of solutions, dashed lines, imaginary parts.

Note that while the time integral of $C(t)$ vanishes for any finite m_0/m , it is nonvanishing in the ordered limit of (16). The frequencies ω_1 and λ also approach finite limits, while $\omega_0 \rightarrow 0$. The electric field autocorrelation function is obtained from (12) and (13), with the simpler results,

$$C(t) = (Z_+ - Z_-)^{-1} \{ (\lambda + Z_+) e^{Z_+ t} - (\lambda + Z_-) e^{Z_- t} \}, \quad (17)$$

$$Z_{\pm} = \frac{1}{2} \lambda - \{ 1 \pm [1 - 4(\omega_1/\lambda)^2]^{1/2} \}. \quad (18)$$

This analysis suggests that for $m_0/m \sim 1$ the mass dependence is dominated by ω_0 , proceeding from oscillatory at small mass ratios (large ω_0) to overdamped at larger mass ratios (small ω_0). However, the infinite mass limit can be either oscillatory or purely damped depending on the coupling parameters Γ and q_0/q , as indicated in (18). This complex behavior of the modes is illustrated in Fig. 8 for $\Gamma = 0.2$ and $q_0/q = 20$. These values correspond to strong coupling ($q_0\Gamma/q = 4$) and large ω_0 when $m_0/m = 1$. Thus at small m_0/m there are two complex conjugate modes and one real mode. As m_0/m increases the modes become overdamped with three real modes. Finally, because of the strong coupling the large mass limit crosses over again to a pair of complex conjugate modes; the third real mode vanishes in this limit.

IV. DISCUSSION

The simple model for electric field dynamics presented here is based on the exact representation (5) for impurity ion velocity response, $D(t)$, as that for a viscoelastic medium. The approximation (7) provides a practical expression in terms of the oscillation frequency ω_0 , the effective damping constant γ , and the viscoelastic relaxation time $\tau = \lambda^{-1}$. These parameters are fixed by the first four time derivatives of $D(t)$ and its time integral (diffusion constant). The elec-

TABLE II. Diffusion coefficients found from the disconnected approximation (D_*^{DA}) and molecular dynamics (MD) simulations (D_*^{MD}) for the plasma conditions $\Gamma = 5$ and $\kappa = 1$. Impurity mass $m_0 = \infty$.

q_0/q	D_*^{DA}	D_*^{MD}
0.2	1.143	1.19
0.5	0.463	0.448
1	0.277	0.248
2	0.202	0.157

tric field autocorrelation function follows directly as the second derivative and therefore is governed by the same three modes. The qualitative behavior of these modes and the electric field autocorrelation function is as follows. When the viscous relaxation time τ is small (small Γ and q_0/q) the correlation function is dominated by two exponentials according to (10). Under these same conditions γ/ω_0 can be large and the two exponentials give real positive decay at short times crossing over to real negative decay at larger times. At the opposite extreme of large Γ and q_0/q , the damping is weak and two of the modes are complex conjugate pairs leading to oscillatory behavior in $C(t)$.

Since this model appears to provide a semiquantitative description of the electric field dynamics, it can be used to interpret and extract information from computer simulation data. For example, it is possible to treat the self-diffusion coefficient as a free parameter to fit the model to the data, and hence determine the diffusion coefficient. In principle, this is better done using the velocity autocorrelation function and the Green-Kubo relation (8). However, as seen in Figs. 2 and 3, the velocity autocorrelation function is slowly decaying and its time integral requires long simulation times. Alternatively, D can be determined *approximately* as a fitting parameter to match the model to the shorter time simulation data for $C(t)$. Since the model is not exact, the diffusion coefficient determined in this way is only an estimate. We have applied this approach for conditions under which we expect the disconnected approximation to be accurate and found good agreement. As the interval over which the best fit is determined is not prescribed, we have also considered determination of D from the time t_0 at which $C(t)$ first vanishes. Such a point always exists since the time integral of $C(t)$ vanishes. The analytic expression for $C(t_0, D) = 0$ from our model is solved for D using t_0 from simulation data. Table II (see also Fig. 9) shows a comparison of results obtained in this way with those from the disconnected approximation for several values of q/q_0 at $\Gamma = 5$. The agreement is quite reasonable. The value of this approach lies in conditions for which the disconnected approximation cannot be trusted and for which simulation times would be prohibitively large. In many applications (e.g., spectral line broadening by complex atoms [17]) only estimates of field relaxation times are important. It is tempting to choose t_0 as the characteristic time for $C(t)$. However, it is seen from (8) that $\beta m_0 D$ is the characteristic time for $D(t)$, and consequently gives a correlation time for $C(t)$ as well. When it is significantly larger than t_0 (e.g., strong coupling), $\beta m_0 D$ provides the proper time scale and our model provides a simple means for its calculation from simulation data.

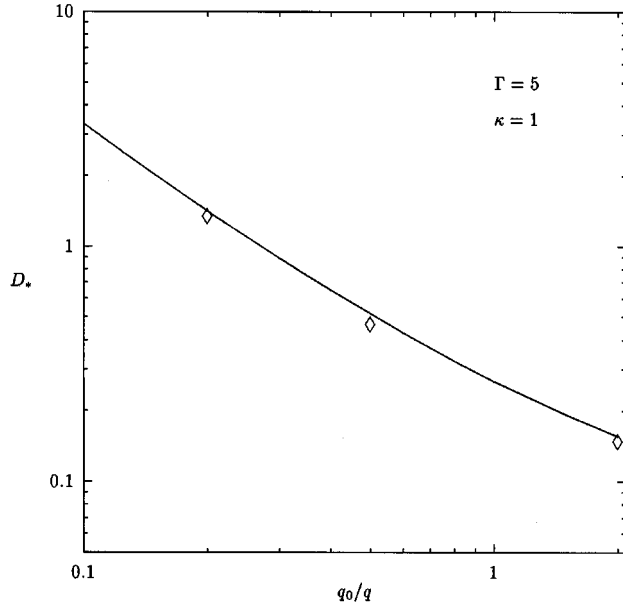


FIG. 9. Diffusion coefficient as a function of q_0/q for plasma coupling $\Gamma=5$ and screening parameter $\kappa=1$. Points: values of D_* found from MD simulations.

ACKNOWLEDGMENTS

The research of J.W.D and M.B. was supported by National Science Foundation Grant No. PHY 9312723. Also, J.W.D. is grateful to the Universite de Provence for its support and hospitality.

APPENDIX A: DERIVATION OF THE MODEL

Formally exact equations for the correlation matrix constructed from the impurity ion velocity \mathbf{v}_0 and the electric field \mathbf{E} can be derived by the projection operator method. This method is described in detail elsewhere [18,15] so only the features relevant for the present application are given here.

Let y_α denote the matrix whose components are \mathbf{v}_0 and \mathbf{E} ,

$$y_\alpha \Rightarrow (\mathbf{v}_0, \mathbf{E}). \quad (\text{A1})$$

A projection operator P is defined for arbitrary phase function X by

$$PX \equiv y_\alpha g_{\alpha\beta}^{-1} \langle y_\beta X \rangle, \quad g_{\alpha\beta} \equiv \langle y_\alpha y_\beta \rangle, \quad (\text{A2})$$

where a summation over repeated Greek labels is assumed, and the brackets denote an equilibrium Gibbs ensemble average. The matrix of correlation functions is defined by

$$C_{\alpha\beta}(t) \equiv \langle y_\alpha(t) y_\beta \rangle. \quad (\text{A3})$$

The dot in (A3) denotes a vector product of the associated elements of y_α . The dynamics of $y_\alpha(t)$ is generated by the Liouville operator L ,

$$y_\alpha(t) \equiv e^{Lt} y_\alpha, \quad LX \equiv \{X, H\}. \quad (\text{A4})$$

Here H is the Hamiltonian and $\{, \}$ denotes Poisson brackets (the corresponding quantum generalization is obtained in a

straightforward manner). The projection operator method then leads to the following exact equations for $C_{\alpha\beta}(t)$:

$$\frac{\partial}{\partial t} C_{\alpha\beta}(t) + \Omega_{\alpha\sigma} C_{\sigma\beta}(t) + \int_0^t d\tau M_{\alpha\sigma}(t-\tau) C_{\sigma\beta}(\tau) = 0, \quad (\text{A5})$$

$$\Omega_{\alpha\beta} = \langle y_\alpha L y_\beta \rangle g_{\beta\beta}^{-1}, \quad M_{\alpha\beta}(t) = \langle (L y_\alpha) e^{QLQ^t} L y_\beta \rangle g_{\beta\beta}^{-1}, \quad (\text{A6})$$

with $Q \equiv 1 - P$ in the last equality.

These results simplify considerably for the choice (A1) made here,

$$g_{\alpha\beta} = \delta_{\alpha\beta} g_{\alpha\alpha}, \quad g_{11} = \langle v_0^2 \rangle, \quad g_{22} = \langle E^2 \rangle, \quad (\text{A7})$$

$$\Omega_{11} = \Omega_{22} = 0, \quad \Omega_{12} = -q_0/m_0, \quad (\text{A8})$$

$$\Omega_{21} = (q_0/m_0) \langle E^2 \rangle / \langle v_0^2 \rangle,$$

$$M_{11}(t) = M_{12}(t) = M_{21}(t) = 0. \quad (\text{A9})$$

The proof of these results is straightforward and will not be given here. The formal equations (A5) now become

$$\frac{\partial}{\partial t} C_{1\beta}(t) = (q_0/m_0) C_{2\beta}(t),$$

$$\frac{\partial}{\partial t} C_{2\beta}(t) + (m_0 \omega_0^2 / q_0) C_{1\beta}(t) + \int_0^t d\tau M_{22}(t-\tau) C_{2\beta}(\tau) = 0, \quad (\text{A10})$$

where $\omega_0^2 \equiv q_0^2 \langle E^2 \rangle / m_0^2 \langle v_0^2 \rangle$. Substituting the first equation of (A10) into the second leads to

$$\left(\frac{\partial^2}{\partial t^2} + \omega_0^2 \right) D(t) + \int_0^t d\tau M(t-\tau) \frac{\partial}{\partial \tau} D(\tau) = 0. \quad (\text{A11})$$

This is the equation used in Sec. II, with the definitions $D(t) \equiv \langle \mathbf{v}(t) \cdot \mathbf{v}_0 \rangle / \langle v_0^2 \rangle$ and $M(t) \equiv M_{22}(t)$. The initial value, $M(0)$, given in (6) follows directly from the definition (A6).

APPENDIX B: EVALUATION OF ω_0 AND ω_1

Consider first ω_0 defined by (6),

$$\omega_0^2 = (\beta q_0^2 / 3m_0) \langle E^2 \rangle = -(\beta q_0 / 3m_0) \langle \mathbf{E} \cdot \nabla_0 U \rangle, \quad (\text{B1})$$

where U is the potential energy of interaction between the impurity ion and the surrounding plasma. This same potential energy also occurs in the Gibbs distribution so the potential energy term in (B1) can be represented by the gradient operating on the Gibbs distribution. Then an integration by parts gives

$$\omega_0^2 = -(q_0 / 3m_0) \langle \nabla_0 \cdot \mathbf{E} \rangle. \quad (\text{B2})$$

At this point a distinction must be made between the cases of Coulomb and screened Coulomb interactions. For the Coulomb case there is a contribution to (B2) from the background field whereas this is zero for the screened case,

$$\nabla_0 \cdot \mathbf{E}_b = - \sum_{\alpha} 4 \pi n_{\alpha} q_{\alpha} \quad (\text{Coulomb}), \quad (\text{B3})$$

$$\nabla_0 \cdot \mathbf{E}_b = 0 \quad (\text{screened}). \quad (\text{B4})$$

Then (B1) leads to the two results

$$\omega_0^2 = \frac{1}{3} \sum_{\alpha} 4 \pi n_{\alpha} q_{\alpha} q_0 / m_0 \quad (\text{Coulomb}), \quad (\text{B5})$$

$$\omega_0^2 = - \frac{1}{3} \sum_{\alpha} (n_{\alpha} q_0 / m_0) \int d\mathbf{r} \nabla \cdot \mathbf{e}_{\alpha}(\mathbf{r}) g_{\alpha}(r) \quad (\text{screened}), \quad (\text{B6})$$

where $g_{\alpha}(r)$ is the radial distribution function for the probability to find a plasma ion of species α at a distance r from the impurity ion. This contribution vanishes for the Coulomb case since $\nabla \cdot \mathbf{e}_{\alpha}(r)$ is proportional to a δ function at $\mathbf{r}=0$ in the Coulomb case and $g_{\alpha}(0)=0$. The above results hold in the thermodynamic limit.

Consider next the frequency ω_1 defined by (6),

$$\omega_1^2 = (\beta q_0^2 / 3 m_0 \omega_0^2) \langle E^2 \rangle = (q_0^2 / 3 m_0 \omega_0^2) \{ \langle [\partial E_i / \partial r_{0j}]^2 \rangle \} + \sum_{\alpha} \sum_{k=1}^{N_{\alpha}} (m_0 / m_{\alpha}) \langle [\partial e_{\alpha i}(\mathbf{r}_k - \mathbf{r}_0) / \partial r_{0j}]^2 \rangle. \quad (\text{B7})$$

To evaluate the first term on the right side of (B7) write the field as $\mathbf{E} = \mathbf{E}' + \mathbf{E}_b$ and note that the uniform background is isotropic, $\partial E_{bi} / \partial r_{0j} = \frac{1}{3} \delta_{ij} \nabla_0 \cdot \mathbf{E}_b$, so

$$\langle [\partial E_i / \partial r_{0j}]^2 \rangle = \langle [\partial E'_i / \partial r_{0j}]^2 \rangle + (\nabla_0 \cdot \mathbf{E}_b)^2 + 2(\nabla_0 \cdot \mathbf{E}_b) \langle \nabla_0 \cdot \mathbf{E}' \rangle.$$

Use of (B2) for the Coulomb case then gives

$$\langle [\partial E_i / \partial r_{0j}]^2 \rangle = \langle [\partial E'_i / \partial r_{0j}]^2 \rangle + 3(m_0 \omega_0^2 / q_0)^2. \quad (\text{B8})$$

With this result (B7) becomes

$$\omega_1^2 = \omega_0^2 + (q_0^2 / 3 m_0^2 \omega_0^2) \sum_{\alpha} (n_{\alpha} m_0 / \mu_{\alpha}) \int d\mathbf{r} [\partial e_{\alpha i}(\mathbf{r}) / \partial r_j]^2 g_{\alpha}(r) + (q_0^2 / 3 m_0^2 \omega_0^2) \sum_{\alpha} \sum_{\sigma} n_{\alpha} n_{\sigma} \int d\mathbf{r} d\mathbf{r}' [\partial e_{\alpha i} / \partial r_j][\partial e_{\sigma i} / \partial r] \times \{ g_{\alpha\sigma}^{(3)}(\mathbf{r}, \mathbf{r}') - g_{\alpha}(r) g_{\sigma}(r') \}, \quad (\text{B9})$$

where $\mu_{\alpha} \equiv m_0 m_{\alpha} / (m_0 + m_{\alpha})$ is the reduced mass.

Repeating this analysis for the screened Coulomb case leads to

$$\omega_1^2 = (q_0^2 / 3 m_0^2 \omega_0^2) \sum_{\alpha} (n_{\alpha} m_0 / \mu_{\alpha}) \int d\mathbf{r} [\partial e_{\alpha i}(\mathbf{r}) / \partial r_j]^2 g_{\alpha}(r) + (9 \omega_0^2)^{-1} \left\{ \sum_{\alpha} (n_{\alpha} q_0 / m_0) \int d\mathbf{r} \nabla \cdot \mathbf{e}_{\alpha}(\mathbf{r}) g_{\alpha}(r) \right\}^2 + (q_0 / 3 m_0 \omega_0)^2 \sum_{\alpha} \sum_{\sigma} n_{\alpha} n_{\sigma} \int d\mathbf{r} d\mathbf{r}' [\partial e_{\alpha i} / \partial r_j][\partial e_{\sigma i} / \partial r] \{ g_{\alpha\sigma}^{(3)}(\mathbf{r}, \mathbf{r}') - g_{\alpha}(r) g_{\sigma}(r') \}.$$

The second term can be simplified using (B6) to give the final result,

$$\omega_1^2 = \omega_0^2 + (q_0^2 / 3 m_0^2 \omega_0^2) \sum_{\alpha} (n_{\alpha} m_0 / \mu_{\alpha}) \int d\mathbf{r} [\partial e_{\alpha i}(\mathbf{r}) / \partial r_j]^2 g_{\alpha}(r) + (q_0^2 / 3 m_0^2 \omega_0^2) \sum_{\alpha} \sum_{\sigma} n_{\alpha} n_{\sigma} \int d\mathbf{r} d\mathbf{r}' [\partial e_{\alpha i} / \partial r_j][\partial e_{\sigma i} / \partial r] \times \{ g_{\alpha\sigma}^{(3)}(\mathbf{r}, \mathbf{r}') - g_{\alpha}(r) g_{\sigma}(r') \} \quad (\text{screened}). \quad (\text{B10})$$

Thus the functional dependence of ω_1 on the fields and ω_0 is the same for Coulomb and screened Coulomb cases.

These results are still exact. The calculations of the text are based on two approximations. The first is neglect of the last term in (B9) and (B10). The second is the use of the HNC integral equation to evaluate the radial distribution function. Furthermore, attention is limited to a one component plasma. In this case (B5) and (B6) can be written

$$\omega_0^2 = \frac{1}{3} \left(\frac{m q_0}{m_0 q} \right) \omega_p^2 I_0, \quad (\text{B11})$$

$$I_0 \equiv 1 + \int_0^{\infty} dr r \kappa^2 e^{-\kappa r} [g(r) - 1], \quad \omega_p^2 \equiv 4 \pi n q^2 / m, \quad (\text{B12})$$

which applies for both the Coulomb ($\kappa=0$) and the screened ($\kappa \neq 0$) cases. Similarly, (B9) and (B10) become

$$\omega_1^2 = \omega_0^2 \{ 1 + (m_0 / \mu I_0^2) I_1 \}, \quad (\text{B13})$$

$$I_1 \equiv \int_0^{\infty} dr r^{-4} e^{-2\kappa r} [6 + 12\kappa r + 10(\kappa r)^2 + 4(\kappa r)^3 + (\kappa r)^4] g(r). \quad (\text{B14})$$

It is understood that the integration variables and screening length κ^{-1} of (B12) and (B14) are in units of the ion sphere radius, $a \equiv (3/4\pi n)^{1/3}$. With these results, the expression (9) for λ becomes

$$\lambda = I_1 / (\beta \mu D I_0^2). \quad (\text{B15})$$

APPENDIX C: EVALUATION OF D

The self-diffusion coefficient is given in terms of the velocity autocorrelation function (8). The model described in Sec. II for $D(t)$ cannot be used to calculate D since (8) yields an identity in that case, by construction. Instead, an approximate kinetic theory is used to obtain the self-diffusion coefficient independently.

The kinetic theory is introduced by representing the velocity autocorrelation function as

$$D(t) = \int d\mathbf{v}_0 \phi(v_0) \mathbf{v}_0 \cdot \mathbf{F}(\mathbf{v}_0, t), \quad (\text{C1})$$

where $\phi_0(v_0)$ is the Maxwell-Boltzmann distribution and $\mathbf{F}(\mathbf{v}_0, t)$ obeys the first Bogoliubov-Born-Green-Kirkwood-Yuon (BBGKY) hierarchy equation with $\mathbf{F}(\mathbf{v}_0, 0) = \mathbf{v}_0$. The projection operator method can be used to obtain a formally exact kinetic equation for \mathbf{F} in the form

$$\frac{\partial}{\partial t} \mathbf{F}(\mathbf{v}_0, t) = \int_0^t d\tau \hat{K}(t-\tau) \mathbf{F}(\mathbf{v}_0, \tau) = 0. \quad (\text{C2})$$

Here $\hat{K}(t)$ is the collision operator, and is an operator over functions of \mathbf{v}_0 ,

$$\hat{K}(t)f(\mathbf{v}_0) \equiv \int d\mathbf{v} K(t; \mathbf{v}_0, \mathbf{v}) f(\mathbf{v}). \quad (\text{C3})$$

The projection operator method provides the form of the function, but it is not required at this point. The self-diffusion coefficient can be expressed in terms of $\hat{K}(t)$ by Laplace transformation of (C3) and use of (C1) in (8),

$$D = \frac{1}{3} \int d\mathbf{v}_0 \phi(v_0) \mathbf{v}_0 \cdot \mathbf{V}(\mathbf{v}_0), \quad (\text{C4})$$

where $\mathbf{V}(\mathbf{v}_0)$ is the solution to the integral equation,

$$\tilde{K}(0) \mathbf{V}(\mathbf{v}_0) = \mathbf{v}_0, \quad \tilde{K}(z) \equiv \int_0^\infty dt e^{-zt} \hat{K}(t). \quad (\text{C5})$$

Thus the Laplace transform of the formal collision operator determines the self-diffusion coefficient.

These results are still exact. We now introduce two types of approximations. The first is an approximate evaluation of D in terms of matrix elements of the $\tilde{K}(0)$. To be more explicit consider the expansion of $\mathbf{V}(\mathbf{v}_0)$ in terms of a complete set of functions $\{\psi_\sigma\}$,

$$\mathbf{V}(\mathbf{v}_0) = \sum_{\sigma}^{\infty} \psi_{\sigma}(\mathbf{v}_0) (\psi_{\sigma}, \mathbf{V}),$$

$$(a, b) \equiv \int d\mathbf{v}_0 \phi(v_0) a^*(\mathbf{v}_0) b(\mathbf{v}_0). \quad (\text{C6})$$

The second expression of (C6) defines the scalar product in the expansion of $\mathbf{V}(\mathbf{v}_0)$. The complete set of functions can be

generated from polynomials in \mathbf{v}_0 using the Schmidt process. The first few are given explicitly by

$$\psi_1(\mathbf{v}_0) = 1, \quad \psi_2(\mathbf{v}_0) = 6^{1/2} [\beta m_0 v_0^2 - 3],$$

$$\psi_i(\mathbf{v}_0) = (\beta m_0)^{1/2} v_{0i} \quad (i = 3, 4, 5). \quad (\text{C7})$$

If only these first five functions of $\{\psi_\sigma\}$ are retained in the representation (C6), then (C4) and (C5) lead directly to the first approximation for D ,

$$\beta m_0 D \rightarrow K_{33}^{-1}, \quad K_{33} \equiv (\psi_3, \tilde{K}(0) \psi_3). \quad (\text{C8})$$

An improvement is obtained by retaining the first eight functions, but the analysis here has been limited to this simplest first approximation, (C8).

Our second approximation refers to the collision operator $\tilde{K}(0)$. Here we use the "disconnected approximation" [9] known to be quite accurate for both neutral and charged fluids even under conditions of strong coupling. In this approximation K_{33} is given by

$$\tilde{K}_{33} = (6\pi m_0)^{-1} \int_0^\infty dk k^4 \tilde{v}_0(k) c_0(k)$$

$$\times \int_{-\infty}^\infty d\omega S(k, \omega) S^{(s)}(k, \omega), \quad (\text{C9})$$

where $S(k, \omega)$ is the dynamic structure factor for density fluctuations in the OCP, $S^{(s)}(k, \omega)$ is the self-structure factor for the impurity ion, $\tilde{v}_0(k)$ is the Fourier transformed pair potential for interaction of the impurity with an ion of the OCP, and $\tilde{c}_0(k)$ is the corresponding Fourier transformed direct correlation function. The corresponding self-diffusion coefficient in this approximation is

$$D^{-1} = (\beta/6\pi)^{-1} \int_0^\infty dk k^4 \tilde{v}(k) c(k)$$

$$\times \int_{-\infty}^\infty d\omega S(k, \omega) S^{(s)}(k, \omega). \quad (\text{C10})$$

It remains to specify models for $S(k, \omega)$ and $S^{(s)}(k, \omega)$. The simplest choice for $S(k, \omega)$ applicable at strong coupling is the mean field model,

$$S(k, \omega) = \frac{2}{\beta \rho \omega} \frac{I''(k)}{[1 - \beta^{-1} \tilde{c}(k) I'(k, \omega)]^2 + [\beta^{-1} \tilde{c}(k) I''(k, \omega)]^2}, \quad (\text{C11})$$

where $I'(k, \omega)$ and $I''(k, \omega)$ are the real and imaginary parts of the function,

$$I(k, \omega) \equiv \lim_{\epsilon \rightarrow 0} \beta n \int d\mathbf{v} \phi(v) (-i\omega + i\mathbf{k} \cdot \mathbf{v} + \epsilon)^{-1}. \quad (\text{C12})$$

Finally, a Gaussian approximation that interpolates between the short time free particle limit and the long time diffusion limit is used for $S^{(s)}(k, \omega)$,

$$S^{(s)}(k, \omega) = \int_0^\infty dt \cos(\omega t) \times \exp(-Dk^2 t + Dk^2 \eta^{-1} [1 - e^{-\eta t}]), \quad (\text{C13})$$

where $\eta \equiv 1/\beta m D$. For the conditions considered here results based on (C13) differ very little from those obtained using the ideal gas form for $S_0^{(s)}(k, \omega)$,

$$S_0^{(s)}(k, \omega) \rightarrow \sqrt{\frac{\pi}{\sigma k}} e^{-(\omega/\sigma k)^2}, \quad (\text{C14})$$

where $\sigma^2 = 2/\beta m$.

APPENDIX D: $M_0 \rightarrow \infty$ LIMIT

The electric field autocorrelation function simplifies considerably in the limit of a very massive ion ($m_0/m \gg 1$). This is relevant for an impurity ion in a OCP of electrons. Consider first some exact results that follow from the projection operator formalism of Appendix A for finite m_0 ,

$$\tilde{D}(z) = [z^2 + z\tilde{M}(z) + \omega_0^2]^{-1} [z + \tilde{M}(z)], \quad (\text{D1})$$

$$\tilde{C}(z) = z[z^2 + z\tilde{M}(z) + \omega_0^2]^{-1}. \quad (\text{D2})$$

Here $\tilde{D}(z)$ and $\tilde{C}(z)$ are the Laplace transforms of $D(t)$ and $C(t)$, respectively. The self-diffusion coefficient is related to $\tilde{D}(0)$ through (8),

$$\beta m_0 D = \lim_{z \rightarrow 0} \tilde{D}(z) = \lim_{z \rightarrow 0} \tilde{M}(z)/\omega_0^2, \quad (\text{D3})$$

while $\tilde{C}(0) = 0$. Now consider the limit of $m_0 \rightarrow \infty$ first, followed by $z \rightarrow 0$. In this case $\beta m_0 \omega_0^2 \rightarrow (\beta^2 q_0^2/3) \langle E^2 \rangle$ and (D3) becomes, instead,

$$D = \lim_{z \rightarrow 0} \lim_{m_0 \rightarrow \infty} 3\tilde{M}(z) (\beta^2 q_0^2 \langle E^2 \rangle)^{-1}. \quad (\text{D4})$$

On the other hand, (D2) gives, for the infinite mass limit of the electric field autocorrelation function,

$$\tilde{C}(z) \rightarrow [z + \tilde{M}(z)]^{-1}. \quad (\text{D5})$$

Comparison of (D4) and (D5) shows an alternative Green-Kubo relation that is applicable only for infinite m_0 ,

$$D^{-1} = \beta^2 q_0^2 \langle E^2 \rangle \lim_{z \rightarrow 0} \lim_{m_0 \rightarrow \infty} \tilde{C}(z), \quad (\text{D6})$$

where the order of the limits is important, since $\lim_{z \rightarrow 0} \tilde{C}(z) = 0$ for any finite mass.

For the approximate model here these results translate to

$$\omega_0 = 0, \quad \omega_1^2 = \frac{q_0 I_1}{3q I_0} \omega_p^2, \quad \lambda = \frac{I_1}{\beta m D I_0^2}. \quad (\text{D7})$$

The self-diffusion coefficient in (D7) is obtained from (C10), where the self-structure factor becomes a δ function at $\omega = 0$ in this limit, giving

$$D^{-1} = (\beta/6\pi)^{-1} \int_0^\infty dk k^4 \nu(k) c(k) S(k, 0). \quad (\text{D8})$$

The electric field autocorrelation function is obtained from (14) and (15),

$$C(t) = (Z_+ - Z_-)^{-1} \{(\lambda + Z_+) e^{Z_+ t} - (\lambda + Z_-) e^{Z_- t}\}, \quad (\text{D9})$$

$$Z_\pm = \frac{1}{2} \lambda \{-1 \pm [1 - 4(\omega_1/\lambda)^2]^{1/2}\}. \quad (\text{D10})$$

It is easily verified that

$$C(0) = \int_0^\infty dt C(t) = \lambda/Z_+ Z_- = \lambda/\omega_1^2 = D^{-1} (3q/q_0 \beta m \omega_p^2 I_0). \quad (\text{D11})$$

This is consistent with the Green-Kubo relation (D6).

-
- [1] For a review with references see J. W. Dufty, in *Strongly Coupled Plasmas*, edited by F. J. Rogers and H. E. DeWitt (Plenum, New York, 1987).
- [2] J. W. Dufty and L. Zogaib, in *Strongly Coupled Plasma Physics*, edited by S. Ichimaru (Elsevier Science, New York, 1990).
- [3] J. W. Dufty and L. Zogaib, *Phys. Rev. A* **44**, 2612 (1991).
- [4] A. Alastuey, J. Lebowitz, and D. Levesque, *Phys. Rev. A* **43**, 2673 (1991).
- [5] J. W. Dufty and L. Zogaib, *Phys. Rev. E* **47**, 2958 (1993).
- [6] M. Berkovsky, J. W. Dufty, A. Calisti, R. Stamm, and B. Talin, *Phys. Rev. E* **51**, 4917 (1995).
- [7] A. Brissaud and U. Frisch, *J. Quant. Spectrosc. Radiat. Transfer* **11**, 1767 (1971).
- [8] J.-P. Hansen and I. R. MacDonald, *Theory of Simple Fluids* (Academic Press, New York, 1986).
- [9] J.-P. Hansen and L. Sjogren, *Phys. Fluids* **25**, 617 (1982).
- [10] Since only the ratio q_0/q is considered in our analysis, the choice of q can be chosen such that the electrons are weakly coupled and that their Debye length is equal to the OCP ion sphere radius a . Then in the units used here the screening length for the screened interactions is unity.
- [11] J. W. Dufty and M. Berkovsky, *Nucl. Instrum. and Methods Phys. Res. B* **96**, 626 (1995); and in *Physics of Strongly Coupled Plasmas*, edited by W. D. Kraeft and M. Schlange (World Scientific, Singapore, 1996).
- [12] D. Boercker, C. Iglesias, and J. Dufty, *Phys. Rev. A* **36**, 2254 (1987).
- [13] D. Boercker, in *Spectral Line Shapes 7*, edited by R. Stamm and B. Talin (Nova Science, New York, 1993); in *Spectral Line Shapes 5*, edited by J. Szudy (Ossolineum, Wroclaw, Poland, 1989).

- [14] R. Stamm, B. Talin, E. L. Pollock, and C. A. Iglesias, Phys. Rev. A **34**, 4144 (1986).
- [15] J-P. Boon and S. Yip, *Molecular Hydrodynamics* (Dover, New York, 1991), Chap. 3.
- [16] For an early application of this model to neutral fluids see G. D. Harp and B. J. Berne, Phys. Rev. A **2**, 975 (1970); B.J. Berne and G. D. Harpe, Adv. Chem. Phys. **17**, 63 (1970).
- [17] B. Talin, A. Calisti, L. Godbert, R. Stamm, R. W. Lee, and L. Klein, Phys. Rev. A **51**, 1918 (1995).
- [18] B. J. Berne, in *Statistical Mechanics, Part B*, edited by B. J. Berne (Plenum Press, New York, 1977).